MOCVD growth of β-Ga₂O₃ on (001) Ga₂O₃ substrates

Lingyu Meng¹, Dongsu Yu¹, Hsien-Lien Huang², Chris Chae², Jinwoo Hwang², and Hongping Zhao^{1,2,‡}

¹Department of Electrical and Computer Engineering, The Ohio State University, Columbus, OH 43210, USA

²Department of Materials Science and Engineering, The Ohio State University, Columbus, OH 43210, USA

‡Corresponding Author Email: <u>zhao.2592@osu.edu</u>

Abstract

In this study, we comprehensively investigated the growth of β-Ga₂O₃ on (001) on-axis Ga₂O₃ substrates via metalorganic chemical vapor deposition (MOCVD) using both triethylgallium (TEGa) and trimethylgallium (TMGa) as the Ga precursors. For MOCVD growth with TEGa, group VI/III molar ratio was tuned with different TEGa molar flow rate. The correlation between growth conditions and the surface morphology, growth rate, and electron transport properties of MOCVD-grown (001) β-Ga₂O₃ thin films is comprehensively analyzed. Room temperature mobility of 85 cm²/V·s with carrier concentration of 2.0 x 10¹⁷ cm⁻³ were measured for a film grown using TEGa molar flow rate of 19 µmol/min and VI/III molar ratio of 934. For MOCVD growth of (001) Ga₂O₃ using TMGa, we observed the occurrence of cracking along [010] direction in the grown films, which was found to be closely related to the film thickness and growth rate. The relatively smooth surface morphology of the films with cracks is attributed to the strain relaxation. (001) β-Ga₂O₃ films containing rotation domains with (-401) plane were observed from high resolution x-ray diffraction (XRD) and confirmed with atomic-resolution scanning transmission electron microscopy (STEM) imaging. Under the same growth condition, (001) β-Ga₂O₃ films contain higher carbon concentration as compared to that of the (010) β-Ga₂O₃ films.

Results from this work provide fundamental insights in MOCVD epitaxy of β -Ga₂O₃ on (001) Ga₂O₃ substrates, revealing the opportunities and challenges of MOCVD growth of (001) β -Ga₂O₃ thin films with fast growth rates for high-power electronic device technology.

I. Introduction

Due to its promising fundamental material properties, such as a large energy bandgap (4.8 eV) [1, 2], controllable n-type doping [3–6], and a high predicted breakdown field strength (8 MV/cm) [7], β -Ga₂O₃ has emerged as a promising semiconductor candidate for the development of next-generation high-power electronic devices [8]. Another key advantage of β -Ga₂O₃ over other wide (GaN, SiC) and ultra-wide (diamond, AlN) bandgap semiconductors is the availability of high-quality, single crystalline native substrates with various orientations [9], enabling high quality epitaxy of β -Ga₂O₃ [4–6, 10–28] and β -(Al_xGa_{1-x})₂O₃ alloys [29–37]. While the technology is in its nascent stage, significant strides have been made in creating β -Ga₂O₃-based devices using bulk and epitaxial thin films, such as lateral and vertical field-effect transistors and Schottky barrier diodes (SBDs) with high breakdown voltages surpassing 6 kV [38–41].

SBDs with a vertical fin structure have been documented with a breakdown voltage of 2.89 kV and a Baliga's figure-of-merit (BFOM) of 0.80 GW/cm² (BV²/Ron,sp) [39]. Vertical fin-shaped channel metal-insulator-semiconductor (MIS) field-effect transistors (FinFETs) have been demonstrated with breakdown voltages (BV) exceeding 2 kV [40]. However, the performance of β-Ga₂O₃ power devices remains well below the material's predicted limit. Various techniques have been explored to improve the BV of vertical β-Ga₂O₃ SBDs, including implanted edge termination, field plates, p-NiO_x rings, fin structures, and high-k oxide field plates [42–46]. Despite these efforts, they have not exceeded the traditional GaN or SiC-based SBDs. Challenges in epitaxial

growth of high-quality, thick drift layers with smooth surface morphology and controllable doping persist as key a factor limiting the performance of β-Ga₂O₃ vertical power devices [9].

To develop high-power vertical electronic devices with high reverse breakdown voltage, a thick drift layer with smooth surface morphology and low controllable doping is crucial. This typically requires faster growth rates while maintaining high epilayer quality. Although relatively rapid growth rates for epitaxial β-Ga₂O₃ layers on (010) oriented β-Ga₂O₃ substrates have been achieved using methods such as low-pressure chemical vapor deposition (LPCVD) [14] and metal-organic chemical vapor deposition (MOCVD) [26, 47], thick film growth often leads to three-dimensional (3D) island formation on the growth surface [28, 47], which inevitably cause compromised power device performance, including non-ideal forward transport, trap-assisted leakage, and high on-resistance.

Prior efforts on MOCVD homoepitaxial growth of β -Ga₂O₃ on on-axis (100) β -Ga₂O₃ substrates revealed stacking faults and twin lamellae formation in the epitaxial films [48]. Although introducing suitable miscut angles on the substrates allows step-flow growth of β -Ga₂O₃ thin films on the (100) plane, growth of thick drift layer with fast growth rates still require further development [17]. Primarily, (001) oriented β -Ga₂O₃ substrates have been utilized for the homoepitaxial growth of β -Ga₂O₃ films, achieving rapid growth rates exceeding 10 μ m/h through halide vapor-phase epitaxy (HVPE). [38]. Majority of the existing vertical β -Ga₂O₃ devices, such as Schottky barrier diodes [39, 41–43, 49], p-n heterojunction diodes [46, 50], or metal-insulator-semiconductor (MIS) diodes [51], have been fabricated on (001) β -Ga₂O₃ films due to the availability of thick (001) β -Ga₂O₃ homoepitaxial drift layers.

However, HVPE growth at rapid growth rates tends to result in significant surface roughness, including surface steps and pits, requiring mechanical and chemical-mechanical polishing (CMP)

processes before device fabrication [13, 52]. These processes not only increase the cost but also likely introduce impurities or contaminants onto the polished surface. As compared to other growth methods, MOCVD remains a promising growth technique due to its ability to produce high-quality crystalline thin films with high mobility, low compensation, and reasonable growth rates. While MOCVD growth of β-Ga₂O₃ films on (010) [6, 15, 20, 21, 24–28] and (100) [16–19, 48, 53, 54] oriented β-Ga₂O₃ substrates has been extensively studied, development and understanding of MOCVD epitaxial β-Ga₂O₃ films on (001) β-Ga₂O₃ substrates is still limited.

In this study, we performed a comprehensive investigation on the growth window of MOCVD (001) β -Ga₂O₃, utilizing triethylgallium (TEGa) and trimethylgallium (TMGa) as the gallium precursors. The main purpose of this study is to identify growth conditions that facilitate the high-quality growth of (001) β -Ga₂O₃ epi-film with high electron mobility, smooth surface morphology and thick (001) β -Ga₂O₃ films with fast growth rates.

II. Experimental Section

MOCVD (001) β-Ga₂O₃ thin films were grown in a far injection showerhead reactor with different growth rates by using TEGa and TMGa as the Ga precursors, respectively. Pure oxygen (O₂) was used as O precursor with Argon (Ar) as the carrier gas. N-type doping was achieved using diluted silane source. The chamber pressure was kept constant at 60 Torr. For the samples grown with TEGa, the O₂ flow rate was adjusted between 400 SCCM and 1000 SCCM, while the TEGa molar flow rate ranged from 12 to 31 μmol/min. The growth temperature was set at 880°C. For the samples grown with TMGa, the O₂ flow rate and TMGa molar flow rate were set at 800 SCCM and 58 μmol/min, respectively. The growth temperature was tuned from 850°C to 950°C. The films

were grown on Sn-doped conductive and Fe-doped semi-insulating (001) Ga₂O₃ substrates. The detailed growth parameters can be found in Table 1 and Table 2.

Room temperature Hall measurements were conducted using the Ecopia HMS-3000 Hall effect system to determine carrier concentrations and electron mobilities under a constant magnetic field of 0.975 T. To establish the Van der Pauw geometry required for these measurements, Ti/Au contacts (30/100 nm) were deposited at the sample's four corners and annealed in a N₂ atmosphere at 470 °C for 1 minute. The surface morphology of the thin films was characterized using optical microscopy and field emission (FE) scanning electron microscopy (FESEM, FEI Helios 650), while the growth rates were determined by measuring the thickness of β-Ga₂O₃ films through cross-sectional FESEM imaging of films co-deposited on sapphire substrates. The surface roughness was obtained using atomic force microscopy (AFM, Bruker AXS Dimension Icon). The crystalline quality of the β-Ga₂O₃ films was evaluated using high-resolution X-ray diffraction (HRXRD, Bruker D8 Discover). High-angle annular dark field (HAADF) scanning transmission electron microscopy (STEM) images of the cracking area were obtained using a Thermo Fisher Scientific Titan STEM operated at 300 kV. Quantitative secondary ion mass spectroscopy (SIMS) was used to probe the impurity profiles of carbon (C).

III. Results and Discussions

In the first part, the results from the MOCVD growths of (001) β -Ga₂O₃ thin films using TEGa are discussed. The influence of O₂ flow rates on the surface morphology and charge transport properties of (001) β -Ga₂O₃ films was systematically studied, with the O₂ flow rates ranging from 400 to 1000 SCCM, as detailed in Table 1 (Sample ID: #1, #2, #3).All other growth parameters were kept constant (TEGa molar flow rate at 31 μ mol/min, growth temperature at 880°C, and chamber pressure at 60 torr). The surface morphologies of the β -Ga₂O₃ films grown under these

conditions were comprehensively assessed using FESEM and AFM imaging. Figures 1(a)-(c) show the surface FESEM images of (001) β-Ga₂O₃ films grown at O₂ flow rate of 400, 800, and 1000 SCCM, respectively. All the samples show smooth surface morphology. The corresponding surface AFM images (over a scan area of 5 x 5 µm²) for the films grown with different O₂ flow rate are shown in Figures 1(d)-(f). Overall surface morphologies are similar among these samples. The growth rates were observed to vary with the O₂ flow rate, as detailed in Table 1. Growth rates remained nearly constant (~700 nm/h) for O₂ flow rates of 800 SCCM or higher. However, reducing the flow rate to 400 SCCM slightly increased the growth rate to 813 nm/h, likely due to the suppressed precursor gas phase reaction from the reduced O₂ flow. The room temperature (RT) Hall mobility was also found to be influenced by the O₂ flow rate, as indicated in Table 1. With the same silane flow, the electron concentrations of the films grown with different O₂ flow rate are found to increase as the O₂ flow rate decreases. Relatively higher mobilities were obtained for films grown with lower O₂ flow rate. This effect can be attributed to reduced compensation at lower O₂ flow rates, resulting from suppressed Ga vacancies being formed [55]. The RT mobility of 80 cm²/V.s with carrier concentration of 8 x 10¹⁶ cm⁻³ was measured for the film grown with 400 SCCM of O₂ flow. As the O₂ flow rate increased, a decrease in Hall mobility was observed, suggesting a degradation in crystalline quality.

Using the relatively low O₂ flow rate condition (400 SCCM), the surface morphology, growth rate and charge transport properties of (001) β-Ga₂O₃ films were systematically investigated as a function of the TEGa molar flow rate. The TEGa molar flow rate was varied from 31 μmol/min to 12 μmol/min (Sample ID: #2, #4, #5 in Table 1). The other parameters, including the O₂ flow (400 SCCM), growth temperature (880 °C), and chamber pressure (60 Torr), remained constant. The surface FESEM images of β-Ga₂O₃ films grown with TEGa molar flow rate ranging from 31

μmol/min to 12 μmol/min are shown in Figures 2(a)-(c), respectively. The corresponding surface AFM images are shown in Figures 2(d)-(f), respectively. All the samples show uniform and smooth and similar surface morphologies with RMS roughness values ranging between 7 and 9 nm. Additionally, we explored the relationship between growth rates and various TEGa molar flow rates, as indicated in Table 1. The findings indicate a broad adjustment of growth rates, from 370 to 813 nm/h, in response to TEGa molar flow rates from 12 μmol/min to 31 μmol/min, which indicates the growth rate is still limited by the mass transfer.

The room temperature Hall mobilities of β-Ga₂O₃ films were measured for those grown at different TEGa molar flow rate as shown in Table 1. With the same silane flow, the electron concentrations of the films are found to increase from $8 \times 10^{16} \, \text{cm}^{-3}$ to $3 \times 10^{17} \, \text{cm}^{-3}$ as the TEGa molar flow rate decreases, which is due to the lower growth rate at the lower TEGa molar flow rate. Relatively higher electron mobility of 85 cm²/V.s with carrier concentration of 2 x 10¹⁷ cm⁻³ was obtained at 19 µmol/min TEGa molar flow rate. The higher Hall mobility reveals the higher crystalline quality, corroborated by the film's relatively smooth surface morphology as shown in Figure 2(b). At a low TEGa molar flow rate of 12 µmol/min, we studied the impact of varying O₂ flow rate (from 400 to 1000 sccm) on β-Ga₂O₃ films (Sample IDs: #5, #6, #7 in Table 1). As shown in Figures 3(a)-(d) and Table 1, there were no significant differences in surface morphology or charge transport properties. This suggests that under low TEGa flow rate conditions, the O₂ flow rate does not significantly affect the thin film quality. Figure 4 plots the correlation between room temperature electron mobility and carrier concentration for the series of samples mentioned earlier, in comparison to values reported for β-Ga₂O₃ films grown via different growth techniques [4-6,11,13,24-26]. Notably, a sample (Sample #4) with a TEGa molar flow rate of 19 μmol/min and

an O₂ flow rate of 400 SCCM achieved a relatively high room temperature mobility of 85 cm²/V·s at a carrier concentration of 2 x 10^{17} cm⁻³.

As compared to TEGa, TMGa is characterized by its higher vapor pressure and more rapid reaction kinetics [21, 56, 57]. Previously, we have achieved high-quality (010) β-Ga₂O₃ films with growth rate of 3 μm/h and room temperature mobility as high as 190 cm²/V·s using TMGa as a precursor [26]. In this study, we investigate the growth conditions conducive to producing high-quality (001) β-Ga₂O₃ film growth with fast growth rates. Using our prior growth condition as a baseline condition, in which the O₂ flow rate and TMGa molar flow rate were kept constant at 800 SCCM and 58 µmol/min, respectively. The growth temperature and chamber pressure were kept constant at 950°C and 60 torr, respectively. The surface view FESEM images of β-Ga₂O₃ film (film thickness =9 μm) grown with a growth rate of 3μm/h using TMGa on (001) Sn-doped β-Ga₂O₃ substrate (Sample #8) were shown in Figure 5. As shown in Figure 5(b) and 5(d), the surface is uniform and smooth, which is different from the films grown on (010) Ga₂O₃ substrates [28, 47]. Additionally, the surface also exhibits a smoother surface morphology as compared to (001) Ga₂O₃ films grown using TEGa. However, we observed the existence of cracks along [010] direction as shown in Figure 5(a) and 5(c), which is due to the existence of strains in the (001) β-Ga₂O₃ film. This could also explain the smoother surface morphology compared to samples grown with TEGa, suggesting that the presence of cracks aids in strain relief within the films, resulting in a smoother surface. To further investigate the influence of the growth duration on the surface morphology, the (001) β-Ga₂O₃ films were grown with the same growth rate of 3 μm/h and varied growth duration from 0.5 h to 3 h (Sample IDs: #10, #9, #8 in Table 2). Optical microscopy was used to assess the surface morphology of these films grown with different growth duration. Figures 6(a)-(c) show the low magnitude optical microscopic surface morphology of (001) β-Ga₂O₃ films grown with

TMGa on Sn-doped (001) β -Ga₂O₃ substrates with different growth duration. The density of the cracks obviously increases as the growth duration increases, which can be attributed to the accumulation of the strains as the increase of the film thickness. Noting for the film grown with 0.5 h (1.5 μ m), no cracks were observed from the optical microscopic images. The corresponding surface AFM images with surface RMS values were shown in Figures 6(g)-(i), respectively. The AFM images were taken from the area between the cracks or without the cracks. The surface RMS value slightly increases from 2.56 nm to 3.24 nm as the growth duration increases from 0.5 h to 3 h.

To elucidate the effect of growth temperature on surface morphology, β-Ga₂O₃ films were grown at temperatures of 950°C and 850°C (Sample IDs: #9, #11, #12 in Table 2). The surface morphology was measured via optical microscopy. The optical microscopic images at low (Figures 7(a)-(c)) and high (Figures 7(d)-(f)) magnifications reveal the morphology of β-Ga₂O₃ films grown using TMGa on Sn-doped (001) β-Ga₂O₃ substrates at different growth temperatures. It was observed that the density of the cracks was not significantly influenced by the growth temperature. The corresponding surface AFM images, along with surface RMS values, are shown in Figures 7(g)-(i). These AFM images were captured from areas avoiding the cracks, indicating that the surface RMS value increases with a decrease in growth temperature. Notably, the sample grown for 1 hour at 850°C exhibits a higher RMS value than the one grown for 2 hours at the same temperature, indicating that increased crack formation can lead to a smoother surface through strain relaxation.

Figure 8 presents the XRD ω -2 θ scans of β -Ga₂O₃ films grown on (001) Ga₂O₃ substrates at a growth temperature of 950°C, with growth durations of 0.5 hours and 3 hours, respectively. Both films exhibit high-intensity, distinguishable diffraction peaks corresponding to the (001)

reflections of β -Ga₂O₃. Notably, an additional peak corresponding to the ($\overline{40}1$) plane of β -Ga₂O₃ was also observed in both films.

We used the low angle annular dark field (LAADF) STEM imaging technique to study the cracking behavior of β-Ga₂O₃ films grown with TMGa on (001) Sn-doped β-Ga₂O₃ substrates. Figure 9(a) displays the cross-sectional STEM LAADF image, revealing the formation of straight cracks across both the film and substrate. Closer examination of the cracking characteristics at magnified regions near the surface (red dotted squares) and interface (orange dotted squares) were shown in Figures 9(b) and 9(c), respectively. The width of the cracks was approximately 100 nm, with a depth of over 8 µm. Non-uniform interfaces were observed between the film and substrate, indicating a critical strain field accumulated during the epitaxial crystal growth. Figure 9(d) shows a magnified region in Figure 9(c), and atomic scale details were provided in Figure 9(e). The STEM high angle annular dark field (HAADF) image shows two different crystal structures for film and substrate regions, indicating the crystal rotation from [001] direction to [401] direction, which is agreed with the XRD results shown in Figure 8. The in-plane rotation of crystal domain planes changed the surface energies [58], resulting in the strain accumulation and termination of the epitaxial growth along [001] direction. Lattice reconstruction at the interface was also observed (red arrows) which can lead to the lattice displacement and further support the strain accumulation. This also indicates the different precursor may play a role for stoichiometric film deposition. Furthermore, the observed interfacial lattice reconstruction (red arrows) can lead to lattice displacement and strain accumulations.

Quantitative secondary ion mass spectroscopy (SIMS) was used to probe the background C impurity concentrations in the MOCVD grown (001) β -Ga₂O₃ film with a growth rate of 3 μ m/h, using a TMGa molar flow rate of 58 μ mol/min, at a growth temperature of 950°C and chamber

pressure of 60 torr (Sample #10). Notably, under the same growth condition (3 µm/h growth rate) [59], the C concentration in (001) β-Ga₂O₃ was 1.8 x 10¹⁸ cm⁻³— about 26 times higher than that of the (010) β-Ga₂O₃ films (6.8 x 10¹⁶ cm⁻³). Given that C acts as a charge compensator in β-Ga₂O₃ [59], this might elucidate the challenges in achieving controllable conductive films with low carrier concentration and high mobility on (001) β-Ga₂O₃ substrates as compared to (010) β-Ga₂O₃ substrates. To understand the mechanisms of higher C incorporation in (001) β-Ga₂O₃ as compared to (010) β-Ga₂O₃, we computed the density of gallium (Ga) and oxygen (O) surface atoms on what are considered 'ideal' surfaces without defects. This determination (refer to Table 3) was guided by the crystal structure of β-Ga₂O₃ when observed from [010] and [001] directions, as illustrated in Figure 10 [60]. As shown in Fig. 10, the Ga density is much higher in the in-plane (001) plane as compared to that of the (010) plane. Higher Ga-atom density on (001) plane can be correlated with higher C incorporation. The number of Ga adsorption sites might influence the likelihood of CH₃ adsorption, which leads to higher C incorporation. Specifically, in a step flow growth mode, C absorbed on terraces can be seized by rapidly propagating steps. This trend aligns well with the previous observations in GaAs and GaN films [61, 62].

IV. Conclusions

In this work, we systematically investigated the MOCVD growth of β-Ga₂O₃ on (001) β-Ga₂O₃ substrate with both TEGa and TMGa as Ga precursors. For films grown with TEGa, the surface morphology, growth rate and electron mobility highly depend on the VI/III ratio and the TEGa molar flow rate. For films grown with TMGa and fast growth rates, we observed the cracks formation along the [010] direction for films with several micrometers. The density of the cracks increases as the film thickness increases. The improved smoothness of the film surface

morphology, characterized by the presence of cracks, is attributed to the relaxation of strain within the films. The cracks are correlated with the appearance of the (-401) rotation domains which were evidenced from both XRD and STEM. Under the same growth condition, the impurity carbon concentration in (001) β -Ga₂O₃ is significantly higher than that in (010) β -Ga₂O₃. The results from this study provide insights on MOCVD epitaxy of (001) β -Ga₂O₃ films. Opportunities and challenges co-exist for developing high quality (001) β -Ga₂O₃ thin films for high power electronic devices.

Acknowledgement

The authors thank the financial support from the Air Force Office of Scientific Research FA9550-18-1-0479 (AFOSR, Dr. Ali Sayir), the NSF (Grant No. 2231026, No. 2019753).

Conflict of Interest Statement

On behalf of all authors, the corresponding author states that there is no conflict of interest.

Data Availability

The data that support the findings of this study are available from the corresponding author upon reasonable request.

References:

- (1) Peelaers, H.; Varley, J. B.; Speck, J. S.; Van de Walle, C. G. Structural and Electronic Properties of Ga₂O₃-Al₂O₃ Alloys. *Appl. Phys. Lett.* **2018**, *112*, 242101.
- (2) Tippins, H. H. Optical Absorption and Photoconductivity in the Band Edge of β -Ga₂O₃. *Phys. Rev.* **1965**, *140*, A316–A319.
- (3) Baldini, M.; Albrecht, M.; Fiedler, A.; Irmscher, K.; Klimm, D.; Schewski, R.; Wagner, G. Semiconducting Sn-Doped β-Ga₂O₃ Homoepitaxial Layers Grown by Metal Organic Vapour-Phase Epitaxy. *J. Mater. Sci.* **2016**, *51*, 3650–3656.
- (4) Goto, K.; Konishi, K.; Murakami, H.; Kumagai, Y.; Monemar, B.; Higashiwaki, M.; Kuramata, A.; Yamakoshi, S. Halide Vapor Phase Epitaxy of Si Doped β -Ga₂O₃ and Its Electrical Properties. *Thin Solid Films* **2018**, *666*, 182–184.

- (5) Ahmadi, E.; Koksaldi, O. S.; Kaun, S. W.; Oshima, Y.; Short, D. B.; Mishra, U. K.; Speck, J. S. Ge Doping of β-Ga₂O₃ Films Grown by Plasma-Assisted Molecular Beam Epitaxy. *Appl. Phys. Express* 2017, 10, 041102.
- (6) Zhang, Y.; Alema, F.; Mauze, A.; Koksaldi, O. S.; Miller, R.; Osinsky, A.; Speck, J. S. MOCVD Grown Epitaxial β -Ga₂O₃ Thin Film with an Electron Mobility of 176 cm²/V s at Room Temperature. *APL Mater.* **2019**, *7*, 022506.
- (7) Varley, J. B. First-Principles Calculations of Structural, Electrical, and Optical Properties of Ultra-Wide Bandgap (Al_xGa_{1-x})₂O₃ alloys. *J. Mater. Res.* **2021**, *36*, 4790–4803.
- (8) Green, A. J.; Speck, J.; Xing, G.; Moens, P.; Allerstam, F.; Gumaelius, K.; Neyer, T.; Arias-Purdue, A.; Mehrotra, V.; Kuramata, A.; Sasaki, K.; Watanabe, S.; Koshi, K.; Blevins, J.; Bierwagen, O.; Krishnamoorthy, S.; Leedy, K.; Arehart, A. R.; Neal, A. T.; Mou, S.; Ringel, S. A.; Kumar, A.; Sharma, A.; Ghosh, K.; Singisetti, U.; Li, W.; Chabak, K.; Liddy, K.; Islam, A.; Rajan, S.; Graham, S.; Choi, S.; Cheng, Z.; Higashiwaki, M. β-Gallium Oxide Power Electronics. *APL Mater.* **2022**, *10*, 029201.
- (9) Kuramata, A.; Koshi, K.; Watanabe, S.; Yamaoka, Y.; Masui, T.; Yamakoshi, S. High-Quality β-Ga₂O₃ Single Crystals Grown by Edge-Defined Film-Fed Growth. *Jpn. J. Appl. Phys.* 2016, 55, 1202A2.
- (10) Leedy, K. D.; Chabak, K. D.; Vasilyev, V.; Look, D. C.; Mahalingam, K.; Brown, J. L.; Green, A. J.; Bowers, C. T.; Crespo, A.; Thomson, D. B.; Jessen, G. H. Si Content Variation and Influence of Deposition Atmosphere in Homoepitaxial Si-Doped β -Ga₂O₃ Films by Pulsed Laser Deposition. *APL Mater.* **2018**, *6*, 101102.
- (11) Sasaki, K.; Kuramata, A.; Masui, T.; Villora, E. G.; Shimamura, K.; Yamakoshi, S. Device-Quality β-Ga₂O₃ Epitaxial Films Fabricated by Ozone Molecular Beam Epitaxy. *Appl. Phys. Express* **2012**, *5*, 035502.
- (12) Mauze, A.; Zhang, Y.; Itoh, T.; Ahmadi, E.; Speck, J. S. Sn Doping of (010) β-Ga₂O₃ Films Grown by Plasma-Assisted Molecular Beam Epitaxy. *Appl. Phys. Lett.* **2020**, *117*, 222102.
- (13) Leach, J. H.; Udwary, K.; Rumsey, J.; Dodson, G.; Splawn, H.; Evans, K. R. Halide Vapor Phase Epitaxial Growth of β -Ga₂O₃ and α -Ga₂O₃ Films. *APL Mater.* **2019**, 7, 022504.
- (14) Zhang, Y.; Feng, Z.; Karim, M. R.; Zhao, H. High-Temperature Low-Pressure Chemical Vapor Deposition of β-Ga₂O₃. *J. Vac. Sci. Technol. A* **2020**, *38*, 050806.
- (15) Bhattacharyya, A.; Ranga, P.; Roy, S.; Ogle, J.; Whittaker-Brooks, L.; Krishnamoorthy, S. Low Temperature Homoepitaxy of (010) β -Ga₂O₃ by Metalorganic Vapor Phase Epitaxy: Expanding the Growth Window. *Appl. Phys. Lett.* **2020**, *117*, 142102.
- (16) Baldini, M.; Albrecht, M.; Fiedler, A.; Irmscher, K.; Schewski, R.; Wagner, G. Editors' Choice—Si- and Sn-Doped Homoepitaxial β-Ga₂O₃ Layers Grown by MOVPE on (010)-Oriented Substrates. *ECS J. Solid State Sci. Technol.* **2016**, *6*, Q3040.
- (17) Bin Anooz, S.; Grüneberg, R.; Wouters, C.; Schewski, R.; Albrecht, M.; Fiedler, A.; Irmscher, K.; Galazka, Z.; Miller, W.; Wagner, G.; Schwarzkopf, J.; Popp, A. Step Flow Growth of β -Ga₂O₃ Thin Films on Vicinal (100) β -Ga₂O₃ Substrates Grown by MOVPE. *Appl. Phys. Lett.* **2020**, *116*, 182106.
- (18) Chou, T.-S.; Seyidov, P.; Bin Anooz, S.; Grüneberg, R.; Tran, T. T. V.; Irmscher, K.; Albrecht, M.; Galazka, Z.; Schwarzkopf, J.; Popp, A. Fast Homoepitaxial Growth of (100) β-Ga₂O₃ Thin Films via MOVPE. *AIP Adv.* **2021**, *11*, 115323.
- (19) Chou, T.-S.; Seyidov, P.; Bin Anooz, S.; Grüneberg, R.; Pietsch, M.; Rehm, J.; Tran, T. T. V.; Tetzner, K.; Galazka, Z.; Albrecht, M.; Irmscher, K.; Fiedler, A.; Popp, A. Suppression

- of Particle Formation by Gas-Phase Pre-Reactions in (100) MOVPE-Grown β -Ga₂O₃ Films for Vertical Device Application. *Appl. Phys. Lett.* **2023**, *122*, 052102.
- (20) Alema, F.; Zhang, Y.; Mauze, A.; Itoh, T.; Speck, J. S.; Hertog, B.; Osinsky, A. H₂O Vapor Assisted Growth of β-Ga₂O₃ by MOCVD. *AIP Adv.* **2020**, *10*, 085002.
- (21) Seryogin, G.; Alema, F.; Valente, N.; Fu, H.; Steinbrunner, E.; Neal, A. T.; Mou, S.; Fine, A.; Osinsky, A. MOCVD Growth of High Purity Ga₂O₃ Epitaxial Films Using Trimethylgallium Precursor. *Appl. Phys. Lett.* **2020**, *117*, 262101.
- (22) Alema, F.; Zhang, Y.; Osinsky, A.; Valente, N.; Mauze, A.; Itoh, T.; Speck, J. S. Low Temperature Electron Mobility Exceeding 10^4 cm²/V s in MOCVD Grown β -Ga₂O₃. *APL Mater.* **2019**, 7, 121110.
- (23) Alema, F.; Seryogin, G.; Osinsky, A.; Osinsky, A. Ge Doping of β -Ga₂O₃ by MOCVD. *APL Mater.* **2021**, *9*, 091102.
- (24) Feng, Z.; Bhuiyan, A F M A. U.; Karim, M. R.; Zhao, H. MOCVD Homoepitaxy of Si-Doped (010) β-Ga₂O₃ Thin Films with Superior Transport Properties. *Appl. Phys. Lett.* 2019, 114, 250601.
- (25) Feng, Z.; Bhuiyan, A F M A. U.; Xia, Z.; Moore, W.; Chen, Z.; McGlone, J. F.; Daughton, D. R.; Arehart, A. R.; Ringel, S. A.; Rajan, S.; Zhao, H. Probing Charge Transport and Background Doping in Metal-Organic Chemical Vapor Deposition-Grown (010) β-Ga₂O₃. *Phys. Status Solidi RRL Rapid Res. Lett.* **2020**, *14*, 2000145.
- (26) Meng, L.; Feng, Z.; Bhuiyan, A F M A. U.; Zhao, H. High-Mobility MOCVD β-Ga₂O₃ Epitaxy with Fast Growth Rate Using Trimethylgallium. *Cryst. Growth Des.* **2022**, *22*, 3896–3904.
- (27) Bhattacharyya, A.; Peterson, C.; Itoh, T.; Roy, S.; Cooke, J.; Rebollo, S.; Ranga, P.; Sensale-Rodriguez, B.; Krishnamoorthy, S. Enhancing the Electron Mobility in Si-Doped (010) β-Ga₂O₃ Films with Low-Temperature Buffer Layers. *APL Mater.* **2023**, *11*, 021110.
- Cooke, J.; Ranga, P.; Bhattacharyya, A.; Cheng, X.; Wang, Y.; Krishnamoorthy, S.; Scarpulla, M. A.; Sensale-Rodriguez, B. Sympetalous Defects in Metalorganic Vapor Phase Epitaxy (MOVPE)-Grown Homoepitaxial β-Ga₂O₃ Films. *J. Vac. Sci. Technol. A* **2023**, *41*, 013406.
- (29) Bhuiyan, A F M A. U.; Feng, Z.; Johnson, J. M.; Chen, Z.; Huang, H.-L.; Hwang, J.; Zhao, H. MOCVD Epitaxy of β-(Al_xGa_{1-x})₂O₃ Thin Films on (010) Ga₂O₃ Substrates and N-Type Doping. *Appl. Phys. Lett.* **2019**, *115*, 120602.
- (30) Bhuiyan, A F M A. U.; Feng, Z.; Johnson, J. M.; Huang, H.-L.; Sarker, J.; Zhu, M.; Karim, M. R.; Mazumder, B.; Hwang, J.; Zhao, H. Phase Transformation in MOCVD Growth of (Al_xGa_{1-x})₂O₃ Thin Films. *APL Mater.* **2020**, *8*, 031104.
- (31) Bhuiyan, A F M A. U.; Feng, Z.; Meng, L.; Zhao, H. MOCVD Growth of (010) β-(Al_xGa_{1-x})₂O₃ Thin Films. *J. Mater. Res.* **2021**, *36*, 4804–4815.
- (32) Bhuiyan, A F M A. U.; Feng, Z.; Meng, L.; Fiedler, A.; Huang, H.-L.; Neal, A. T.; Steinbrunner, E.; Mou, S.; Hwang, J.; Rajan, S.; Zhao, H. Si Doping in MOCVD Grown (010) β-(Al_xGa_{1-x})₂O₃ Thin Films. *J. Appl. Phys.* **2022**, *131*, 145301.
- (33) Bhuiyan, A F M A. U.; Feng, Z.; Johnson, J. M.; Huang, H.-L.; Hwang, J.; Zhao, H. MOCVD Epitaxy of Ultrawide Bandgap β-(Al_xGa_{1-x})₂O₃ with High-Al Composition on (100) β-Ga₂O₃ Substrates. *Cryst. Growth Des.* **2020**, *20*, 6722–6730.
- (34) Bhuiyan, A F M A. U.; Feng, Z.; Johnson, J. M.; Huang, H.-L.; Hwang, J.; Zhao, H. MOCVD Growth of β-Phase (Al_xGa_{1-x})₂O₃ on ($\overline{2}01$) β-Ga₂O₃ Substrates. *Appl. Phys. Lett.* **2020**, *117*, 142107.

- (35) Bhuiyan, A F M A. U.; Meng, L.; Huang, H.-L.; Sarker, J.; Chae, C.; Mazumder, B.; Hwang, J.; Zhao, H. Metalorganic Chemical Vapor Deposition of β-(Al_xGa_{1-x})₂O₃ Thin Films on (001) β-Ga₂O₃ Substrates. *APL Mater.* **2023**, *11*, 041112.
- (36) Bhuiyan, A F M A. U.; Meng, L.; Huang, H.-L.; Chae, C.; Hwang, J.; Zhao, H. Al Incorporation up to 99% in Metalorganic Chemical Vapor Deposition-Grown Monoclinic (Al_xGa_{1-x})₂O₃ Films Using Trimethylgallium. *Phys. Status Solidi RRL Rapid Res. Lett.* **2023**, *17*, 2300224.
- (37) Bhuiyan, A F M A. U.; Feng, Z.; Meng, L.; Zhao, H. Tutorial: Metalorganic Chemical Vapor Deposition of β-Ga₂O₃ Thin Films, Alloys, and Heterostructures. *J. Appl. Phys.* **2023**, *133*, 211103.
- (38) Hu, Z.; Zhou, H.; Feng, Q.; Zhang, J.; Zhang, C.; Dang, K.; Cai, Y.; Feng, Z.; Gao, Y.; Kang, X.; Hao, Y. Field-Plated Lateral β-Ga₂O₃ Schottky Barrier Diode With High Reverse Blocking Voltage of More Than 3 kV and High DC Power Figure-of-Merit of 500 MW/cm². *IEEE Electron Device Lett.* 2018, 39, 1564–1567.
- (39) Li, W.; Nomoto, K.; Hu, Z.; Jena, D.; Xing, H. G. Field-Plated Ga₂O₃ Trench Schottky Barrier Diodes With a BV²/R_{on,sp} of up to 0.95 GW/cm². *IEEE Electron Device Lett.* **2020**, 41, 107–110.
- (40) Li, W.; Nomoto, K.; Hu, Z.; Nakamura, T.; Jena, D.; Xing, H. G. Single and Multi-Fin Normally-off Ga₂O₃ Vertical Transistors with a Breakdown Voltage over 2.6 kV. In *2019 IEEE International Electron Devices Meeting (IEDM)*; 2019; p 12.4.1-12.4.4.
- (41) Dong, P.; Zhang, J.; Yan, Q.; Liu, Z.; Ma, P.; Zhou, H.; Hao, Y. 6 KV/3.4 MΩ·cm² Vertical β-Ga₂O₃ Schottky Barrier Diode With BV²/R_{on,sp} Performance Exceeding 1-D Unipolar Limit of GaN and SiC. *IEEE Electron Device Lett.* **2022**, *43*, 765–768.
- (42) Konishi, K.; Goto, K.; Murakami, H.; Kumagai, Y.; Kuramata, A.; Yamakoshi, S.; Higashiwaki, M. 1-kV Vertical Ga₂O₃ Field-Plated Schottky Barrier Diodes. *Appl. Phys. Lett.* **2017**, *110*, 103506.
- (43) Sasaki, K.; Wakimoto, D.; Thieu, Q. T.; Koishikawa, Y.; Kuramata, A.; Higashiwaki, M.; Yamakoshi, S. First Demonstration of Ga₂O₃ Trench MOS-Type Schottky Barrier Diodes. *IEEE Electron Device Lett.* **2017**, *38*, 783–785.
- (44) Lin, C.-H.; Yuda, Y.; Wong, M. H.; Sato, M.; Takekawa, N.; Konishi, K.; Watahiki, T.; Yamamuka, M.; Murakami, H.; Kumagai, Y.; Higashiwaki, M. Vertical Ga₂O₃ Schottky Barrier Diodes With Guard Ring Formed by Nitrogen-Ion Implantation. *IEEE Electron Device Lett.* **2019**, *40*, 1487–1490.
- (45) Zhou, H.; Yan, Q.; Zhang, J.; Lv, Y.; Liu, Z.; Zhang, Y.; Dang, K.; Dong, P.; Feng, Z.; Feng, Q.; Ning, J.; Zhang, C.; Ma, P.; Hao, Y. High-Performance Vertical β-Ga₂O₃ Schottky Barrier Diode With Implanted Edge Termination. *IEEE Electron Device Lett.* 2019, 40, 1788–1791.
- (46) Yan, Q.; Gong, H.; Zhang, J.; Ye, J.; Zhou, H.; Liu, Z.; Xu, S.; Wang, C.; Hu, Z.; Feng, Q.; Ning, J.; Zhang, C.; Ma, P.; Zhang, R.; Hao, Y. β-Ga₂O₃ Hetero-Junction Barrier Schottky Diode with Reverse Leakage Current Modulation and BV²/R_{on,sp} Value of 0.93 GW/cm². *Appl. Phys. Lett.* **2021**, 118, 122102.
- (47) Meng, L.; Bhuiyan, A F M A. U.; Yu, D. S.; Huang, H. L.; Hwang, J.; Zhao, H. MOCVD Growth of Thick β-(Al)GaO Films with Fast Growth Rates. *Cryst. Growth Des.* **2023**, *23*, 7365–7373.
- (48) Schewski, R.; Baldini, M.; Irmscher, K.; Fiedler, A.; Markurt, T.; Neuschulz, B.; Remmele, T.; Schulz, T.; Wagner, G.; Galazka, Z.; Albrecht, M. Evolution of Planar

- Defects during Homoepitaxial Growth of β -Ga₂O₃ Layers on (100) Substrates—A Quantitative Model. *J. Appl. Phys.* **2016**, *120*, 225308.
- (49) Kumar, S.; Murakami, H.; Kumagai, Y.; Higashiwaki, M. Vertical β-Ga₂O₃ Schottky Barrier Diodes with Trench Staircase Field Plate. *Appl. Phys. Express* **2022**, *15*, 054001.
- (50) Zhang, J.; Dong, P.; Dang, K.; Zhang, Y.; Yan, Q.; Xiang, H.; Su, J.; Liu, Z.; Si, M.; Gao, J.; Kong, M.; Zhou, H.; Hao, Y. Ultra-Wide Bandgap Semiconductor Ga₂O₃ Power Diodes. *Nat. Commun.* **2022**, *13*, 3900.
- (51) Li, W.; Nomoto, K.; Hu, Z.; Tanen, N.; Sasaki, K.; Kuramata, A.; Jena, D.; Xing, H. G. 1.5 KV Vertical Ga₂O₃ Trench-MIS Schottky Barrier Diodes. In *2018 76th Device Research Conference (DRC)*; **2018**; pp 1–2.
- (52) Murakami, H.; Nomura, K.; Goto, K.; Sasaki, K.; Kawara, K.; Thieu, Q. T.; Togashi, R.; Kumagai, Y.; Higashiwaki, M.; Kuramata, A.; Yamakoshi, S.; Monemar, B.; Koukitu, A. Homoepitaxial Growth of β-Ga₂O₃ Layers by Halide Vapor Phase Epitaxy. *Appl. Phys. Express* 2014, 8, 015503.
- (53) Schewski, R.; Lion, K.; Fiedler, A.; Wouters, C.; Popp, A.; Levchenko, S. V.; Schulz, T.; Schmidbauer, M.; Bin Anooz, S.; Grüneberg, R.; Galazka, Z.; Wagner, G.; Irmscher, K.; Scheffler, M.; Draxl, C.; Albrecht, M. Step-Flow Growth in Homoepitaxy of β-Ga₂O₃ (100)—The Influence of the Miscut Direction and Faceting. *APL Mater.* **2019**, 7, 022515.
- (54) Meng, L.; Bhuiyan, A F M A. U.; Feng, Z.; Huang, H.-L.; Hwang, J.; Zhao, H. Metalorganic Chemical Vapor Deposition of (100) β-Ga₂O₃ on on-Axis Ga₂O₃ Substrates. J. Vac. Sci. Technol. A 2022, 40, 062706.
- (55) Varley, J. B.; Peelaers, H.; Janotti, A.; Van De Walle, C. G. Hydrogenated Cation Vacancies in Semiconducting Oxides. J. Phys.: Condens. Matter 2011, 23 (33), 334212.
- (56) Thompson, A. G. MOCVD Technology for Semiconductors. *Mater. Lett.* **1997**, *30*, 255–263.
- (57) Larsen, C. A.; Buchan, N. I.; Li, S. H.; Stringfellow, G. B. Decomposition Mechanisms of Trimethylgallium. *J. Cryst. Growth* **1990**, *102*, 103–116.
- (58) Mu, S.; Wang, M.; Peelaers, H.; Van de Walle, C. G. First-Principles Surface Energies for Monoclinic Ga₂O₃ and Al₂O₃ and Consequences for Cracking of (Al_xGa_{1-x})₂O₃. *APL Mater.* **2020**, *8*, 091105.
- (59) Meng, L.; Bhuiyan, A F M A. U.; Zhao, H. The Role of Carbon and C-H Neutralization in MOCVD β-Ga₂O₃ Using TMGa as Precursor. *Appl. Phys. Lett.* **2023**, *122*, 232106.
- (60) Cheng, Z.; Hanke, M.; Galazka, Z.; Trampert, A. Thermal Expansion of Single-Crystalline β-Ga₂O₃ from RT to 1200 K Studied by Synchrotron-Based High Resolution x-Ray Diffraction. *Appl. Phys. Lett.* **2018**, *113*, 182102.
- (61) Kondo, M.; Tanahashi, T. Dependence of Carbon Incorporation on Crystallographic Orientation during Metalorganic Vapor Phase Epitaxy of GaAs and AlGaAs. *J. Cryst. Growth* **1994**, *145*, 390–396.
- (62) Cruz, S. C.; Keller, S.; Mates, T. E.; Mishra, U. K.; DenBaars, S. P. Crystallographic Orientation Dependence of Dopant and Impurity Incorporation in GaN Films Grown by Metalorganic Chemical Vapor Deposition. *J. Cryst. Growth* **2009**, *311*, 3817–3823.

Table Caption

Table 1. Summary of β-Ga₂O₃ films grown on (001) Ga₂O₃ substrates using TEGa with different growth conditions: TEGa molar flow rate (12-31 μmol/min), O₂ flow rate (400-1000 SCCM), and silane molar flow rate (0.11-0.25 nmol/min).

Table 2. Summary of β-Ga₂O₃ films grown on (001) Ga₂O₃ substrates using TMGa with different growth conditions: growth duration (0.5h-3 h), growth temperature (850°C-950°C), and silane molar flow rate (0.11-0.55 nmol/min).

Table 3. The carbon concentration in epitaxial films of different orientations, as determined by SIMS under the same growth conditions, correlates with the atom density on the ideal surfaces of various crystallographic orientations.

Figure Captions

- **Fig 1**. Surface view FESEM images of (001) β-Ga₂O₃ films grown with TEGa at different O₂ flow rate: (a) 400 SCCM (#2), (b) 800 SCCM (#1), and (c) 1000 SCCM (#3). The corresponding surface AFM images (5μm x 5μm scan area) of β-Ga₂O₃ films grown with TEGa at different O₂ flow rate: (d) 400 SCCM (#2), (e) 800 SCCM (#1), and (f) 1000 SCCM (#3). TEGa molar flow rate was set at 31 μmol/min. The growth temperature and chamber pressure were constant at 880°C and 60 Torr, respectively.
- **Fig 2**. Surface view FESEM images of (001) β-Ga₂O₃ films grown with TEGa at different TEGa molar flow rate: (a) 31 μmol/min (#2), (b) 19 μmol/min (#4), and (c) 12 μmol/min (#5). The corresponding surface AFM images (5μm x 5μm scan area) of (001) β-Ga₂O₃ films grown with TEGa at different TEGa molar flow rate: (d) 31 μmol/min (#2), (e) 19 μmol/min (#4), and (f) 12 μmol/min (#5). O₂ flow rate was set at 400 SCCM. The growth temperature and chamber pressure were constant at 880°C and 60 Torr, respectively.
- **Fig 3**. Surface view FESEM images of (001) β-Ga₂O₃ films grown with TEGa at different O₂ flow rate: (a) 400 SCCM (#5) and (b) 1000 SCCM (#7). The corresponding surface AFM images (5μm x 5μm scan area) of (001) β-Ga₂O₃ films grown with TEGa at different O₂ flow rate: (c) 400 SCCM (#5) and (d) 1000 SCCM (#7). TEGa molar flow rate was set at 12 μmol/min. The growth temperature and chamber pressure were constant at 880°C and 60 Torr, respectively.
- Fig 4. Room temperature electron mobility vs. electron concentration for (001) β -Ga₂O₃ homoepitaxial thin films from this study (TEGa). The plot also includes previously published data from various growth techniques. Additionally, the growth rates for each set of data are provided.

Fig 5. Surface view FESEM images of β-Ga₂O₃ film (9 μm) grown with TMGa on (001) Sndoped β- Ga₂O₃ substrate (#8): large field of view of (a) cracking area and (b) no-cracking area; high magnification of (c) cracking area and (d) no-cracking area. The cracks are along [010] direction. The film is grown with a growth rate of 3 μm/hr.

Fig 6. Optical microscopic surface morphology of β-Ga₂O₃ films grown with TMGa on Sndoped (001) β-Ga₂O₃ substrates with different growth duration: (a,d) 3h (#8) (b,e) 2h (#9), and (c,f) 0.5h (#10). All the films are grown with same growth rate of 3 μm/hr. The corresponding surface AFM images (5μm x 5μm scan area) of β-Ga₂O₃ films grown with TMGa on Sn-doped (001) β-Ga₂O₃ substrates with different growth duration: (g) 3h (#8), (h) 2h (#9), and (i) 0.5h (#10).

Fig 7. Optical microscopic surface morphology of β-Ga₂O₃ films grown with TMGa on Sndoped (001) β-Ga₂O₃ substrates with different growth temperature and duration. (a,d) 950°C,2h (#9); (b,e) 850°C,2h (#11); and (c,f) 850°C,1h (#12). The corresponding surface AFM images (5μm x 5μm scan area) of β-Ga₂O₃ films grown with TMGa on Sn-doped (001) β-Ga₂O₃ substrates with different growth temperature and duration. (a) 950°C,2h (#9); (b) 850°C,2h (#11); and (c) 850°C,1h (#12).

Fig 8. XRD ω -2θ patterns for β -Ga₂O₃ films grown with TMGa on (001) Sn-doped β -Ga₂O₃ substrates with different growth duration: (a) 0.5h (#10) and (b) 3h (#8).

Fig 9. High resolution STEM images of β-Ga₂O₃ films grown with TMGa on (001) Sn-doped β-Ga₂O₃ substrate (#9) (a) The cracking in the film (b) zig zag at the interface and (c) high mag zig zag area and (d) rotation domains.

Fig 10. Crystal structure of β-Ga₂O₃ viewed in [010] (left) and [001] (right) directions.

Table 1. Summary of β -Ga₂O₃ films grown on (001) Ga₂O₃ substrates using TEGa with different growth conditions: TEGa molar flow rate (12-31 μ mol/min), O₂ flow rate (400-1000 SCCM), and silane molar flow rate (0.11-0.25 nmol/min).

Sample ID	TEGa molar flow rate (μmol/min)	Oxygen flow (SCCM)	Growth Temperature (°C)	Chamber Pressure (Torr)	Silane molar flow rate (nmol/min)	Growth Duration	Film thickness (nm)	Growth rate (nm/h)	Electron concentration (cm ⁻³)	Hall mobility (cm²/Vs)
#1	31	800	880	60	0.25	45min	510	680	Insulati	ng
#2	31	400	880	60	0.25	45min	610	813	8 x10 ¹⁶	80
#3	31	1000	880	60	0.25	45min	540	720	4.2 x10 ¹⁶	45
#4	19	400	880	60	0.25	45min	406	541	2 x10 ¹⁷	85
#5	12	400	880	60	0.11	45min	278	371	3.1 x10 ¹⁷	47
#6	12	800	880	60	0.11	45min	255	340	4 x10 ¹⁷	69
#7	12	1000	880	60	0.11	45min	233	311	3.9 x10 ¹⁷	59

Table 2. Summary of β -Ga₂O₃ films grown on (001) Ga₂O₃ substrates using TMGa with different growth conditions: growth duration (0.5h-3 h), growth temperature (850°C-950°C), and silane molar flow rate (0.11-0.55 nmol/min).

	TMGa molar flow rate (μmol/min)	Oxygen flow (SCCM)	Growth temperature (°C)	Chamber pressure (Torr)	Silane molar flow rate (nmol/min)	Growth duration	Cooling down duration (950C to 650 C)	Film thickness (um)	Growth rate (um/h)
#8	58	800	950	60	0.11	3h	5min	9.50	3.17
#9	58	800	950	60	0.11	2h	5min	5.70	2.85
#10	58	800	950	60	0.11	0.5h	5min	1.40	2.80
#11	58	800	850	60	0.55	2h	5min	5.90	2.95
#12	58	800	850	60	0.55	1h	5min	2.86	2.86

Table 3. The carbon concentration in epitaxial films of different orientations, as determined by SIMS under the same growth conditions, correlates with the atom density on the ideal surfaces of various crystallographic orientations.

Orientation	[C] (cm ⁻³)	Ga Atoms (x 10 ¹⁵ /cm ²)	O Atoms (x 10 ¹⁵ /cm ²)
(010)	6.8 x 10 ¹⁶	1.19	2.08
(001)	1.8 x 10 ¹⁸	3.40	2.83

Fig 1. Surface view FESEM images of (001) β-Ga₂O₃ films grown with TEGa at different O₂ flow rate: (a) 400 SCCM (#2), (b) 800 SCCM (#1), and (c) 1000 SCCM (#3). The corresponding surface AFM images (5μm x 5μm scan area) of β-Ga₂O₃ films grown with TEGa at different O₂ flow rate: (d) 400 SCCM (#2), (e) 800 SCCM (#1), and (f) 1000 SCCM (#3). TEGa molar flow rate was set at 31 μmol/min. The growth temperature and chamber pressure were constant at 880°C and 60 Torr, respectively.

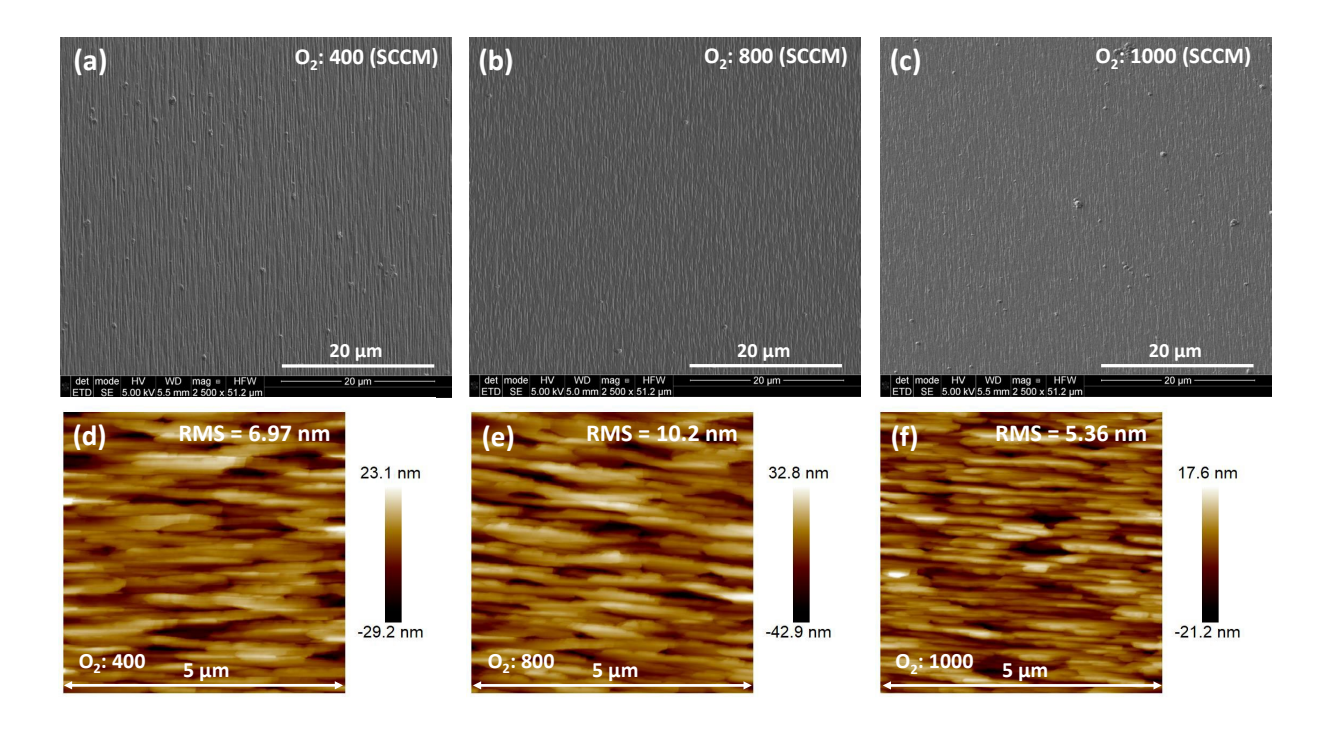


Fig 2. Surface view FESEM images of (001) β-Ga₂O₃ films grown with TEGa at different TEGa molar flow rate: (a) 31 μmol/min (#2), (b) 19 μmol/min (#4), and (c) 12 μmol/min (#5). The corresponding surface AFM images (5μm x 5μm scan area) of (001) β-Ga₂O₃ films grown with TEGa at different TEGa molar flow rate: (d) 31 μmol/min (#2), (e) 19 μmol/min (#4), and (f) 12 μmol/min (#5). O₂ flow rate was set at 400 SCCM. The growth temperature and chamber pressure were constant at 880°C and 60 Torr, respectively.

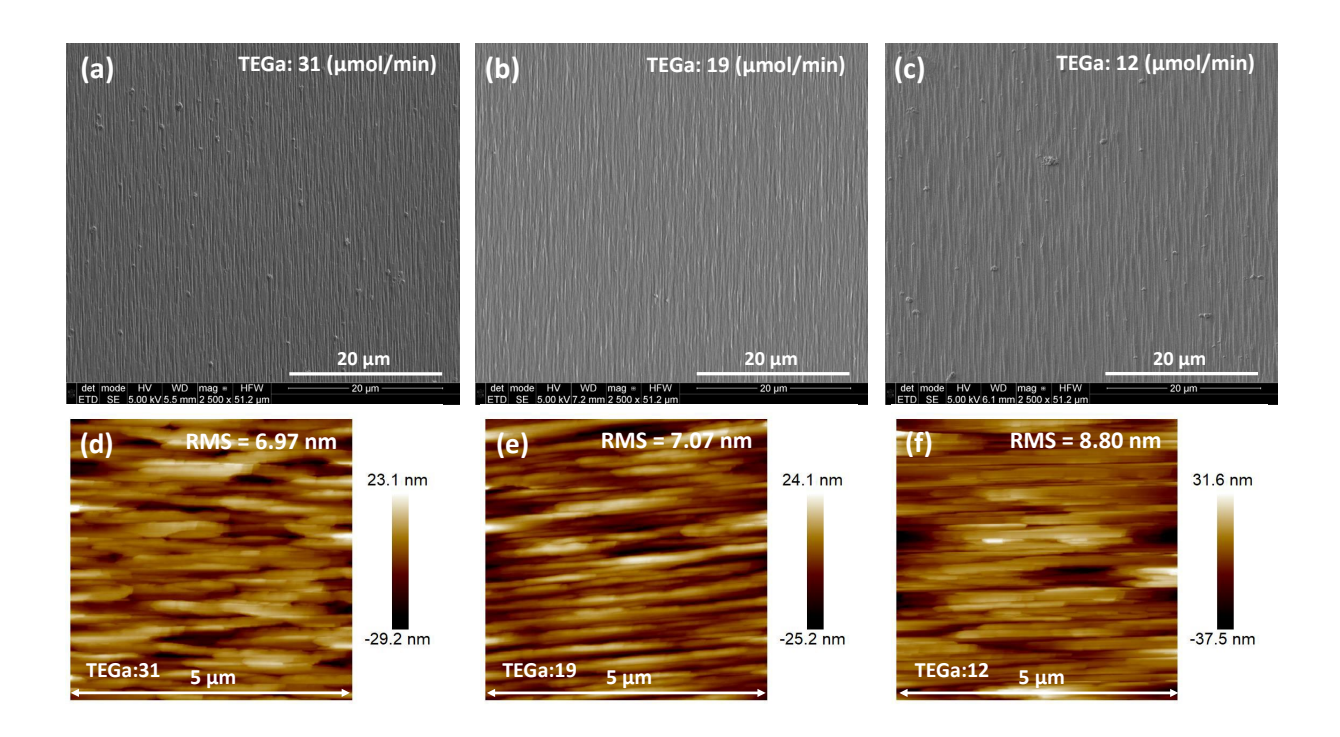


Fig 3. Surface view FESEM images of (001) β-Ga₂O₃ films grown with TEGa at different O₂ flow rate: (a) 400 SCCM (#5) and (b) 1000 SCCM (#7). The corresponding surface AFM images (5μm x 5μm scan area) of (001) β-Ga₂O₃ films grown with TEGa at different O₂ flow rate: (c) 400 SCCM (#5) and (d) 1000 SCCM (#7). TEGa molar flow rate was set at 12 μmol/min. The growth temperature and chamber pressure were constant at 880°C and 60 Torr, respectively.

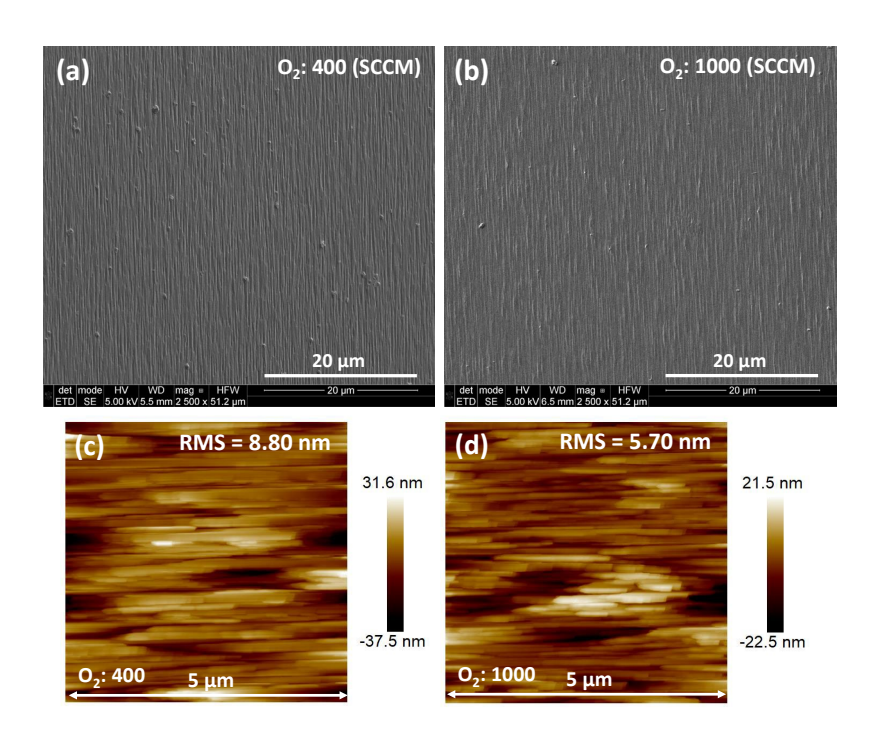


Fig 4. Room temperature electron mobility vs. electron concentration for (001) β -Ga₂O₃ homoepitaxial thin films from this study (TEGa). The plot also includes previously published data from various growth techniques. Additionally, the growth rates for each set of data are provided.

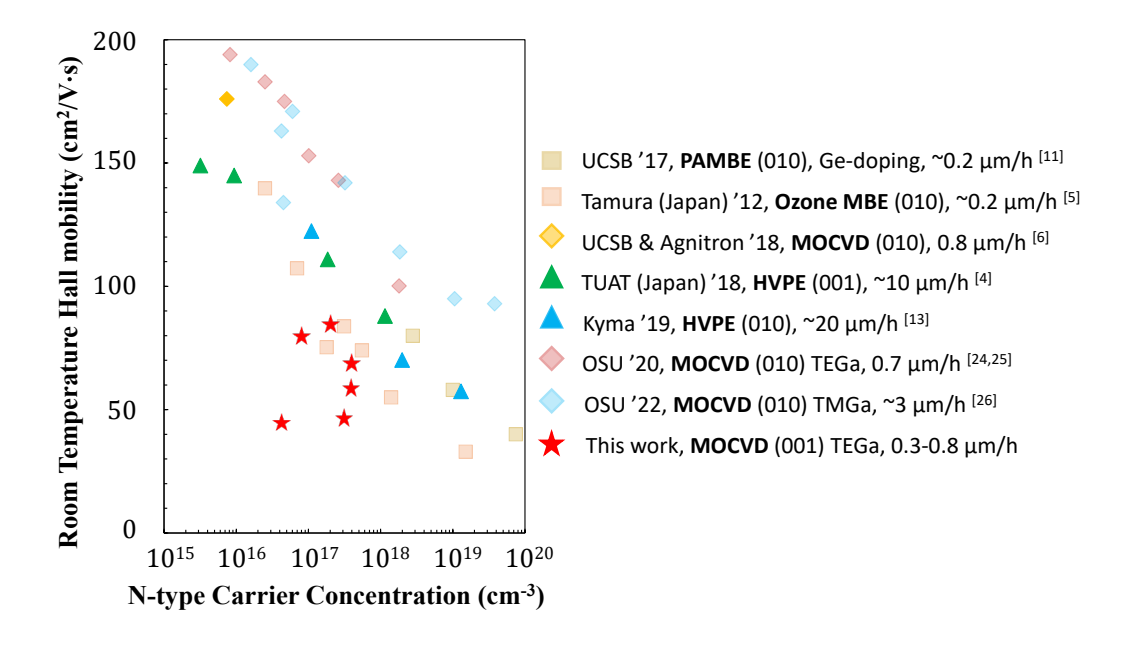


Fig 5. Surface view FESEM images of β-Ga₂O₃ film (9 μm) grown with TMGa on (001) Sndoped β- Ga₂O₃ substrate (#8): large field of view of (a) cracking area and (b) no-cracking area; high magnification of (c) cracking area and (d) no-cracking area. The cracks are along [010] direction. The film is grown with a growth rate of 3 μm/hr.

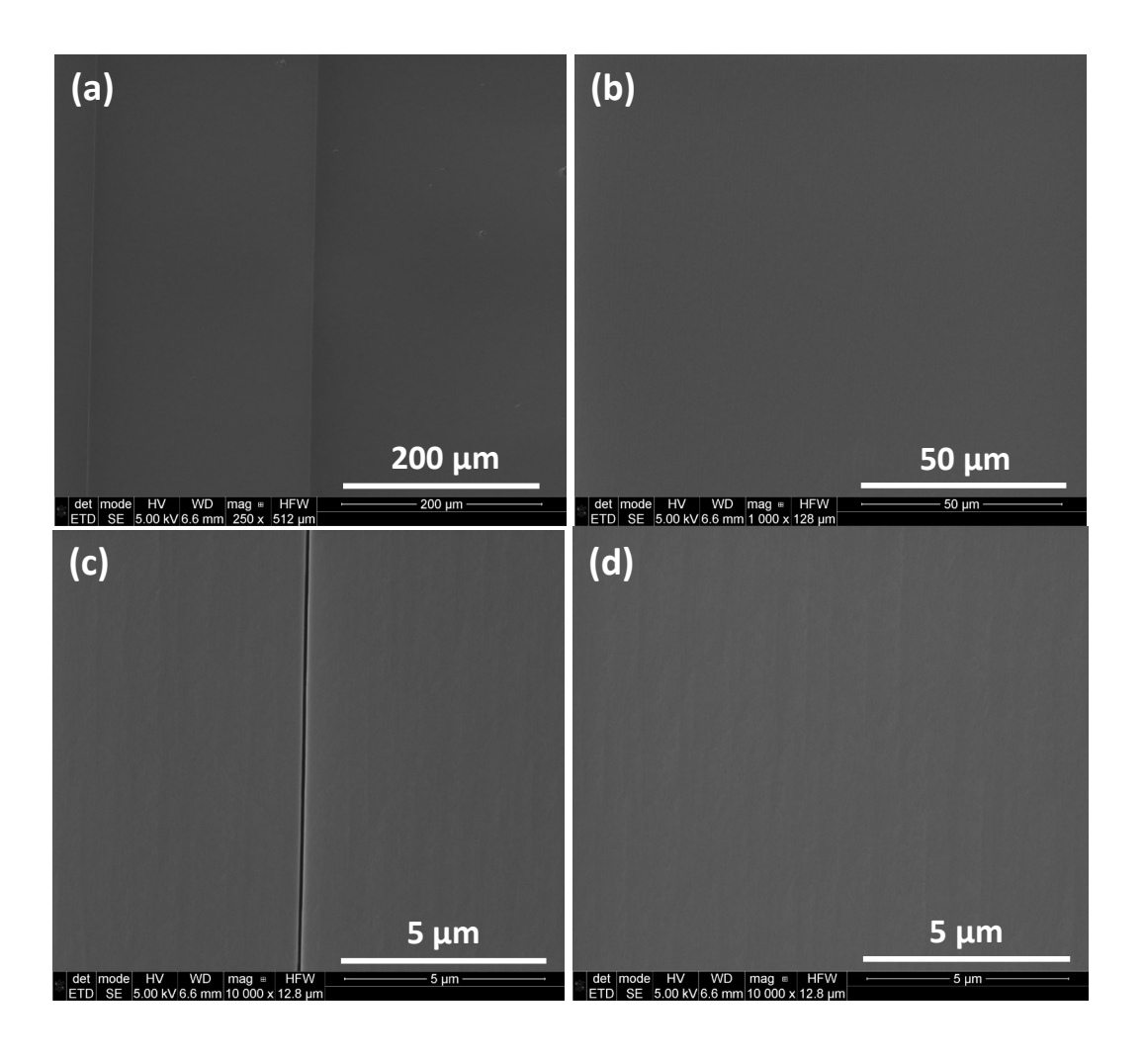


Fig 6. Optical microscopic surface morphology of β-Ga₂O₃ films grown with TMGa on Sndoped (001) β-Ga₂O₃ substrates with different growth duration: (a,d) 3h (#8) (b,e) 2h (#9), and (c,f) 0.5h (#10). All the films are grown with same growth rate of 3 μm/hr. The corresponding surface AFM images (5μm x 5μm scan area) of β-Ga₂O₃ films grown with TMGa on Sn-doped (001) β-Ga₂O₃ substrates with different growth duration: (g) 3h (#8), (h) 2h (#9), and (i) 0.5h (#10).

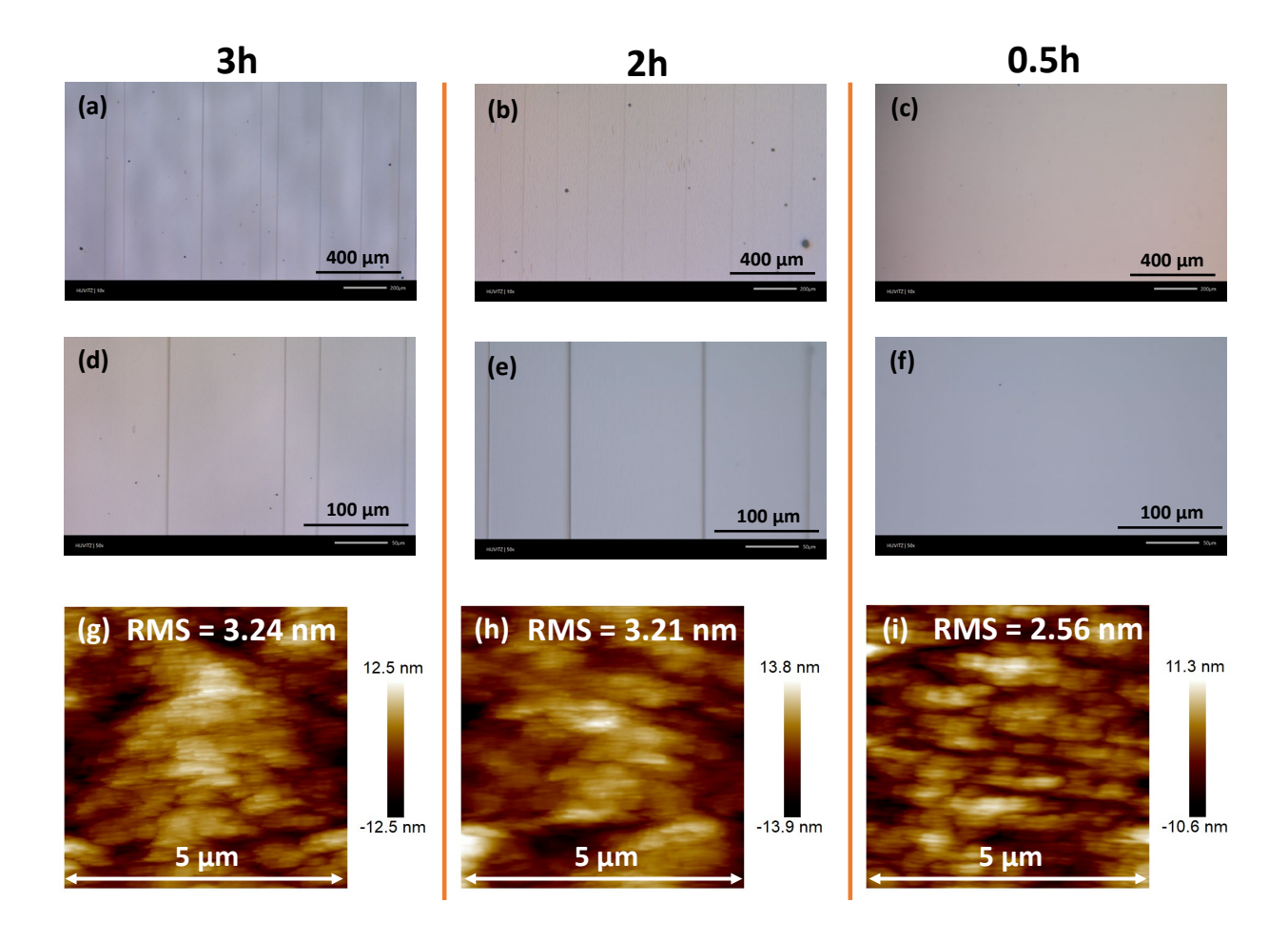


Fig 7. Optical microscopic surface morphology of β-Ga₂O₃ films grown with TMGa on Sndoped (001) β-Ga₂O₃ substrates with different growth temperature and duration. (a,d) 950°C,2h (#9); (b,e) 850°C,2h (#11); and (c,f) 850°C,1h (#12). The corresponding surface AFM images (5μm x 5μm scan area) of β-Ga₂O₃ films grown with TMGa on Sn-doped (001) β-Ga₂O₃ substrates with different growth temperature and duration. (a) 950°C,2h (#9); (b) 850°C,2h (#11); and (c) 850°C,1h (#12).

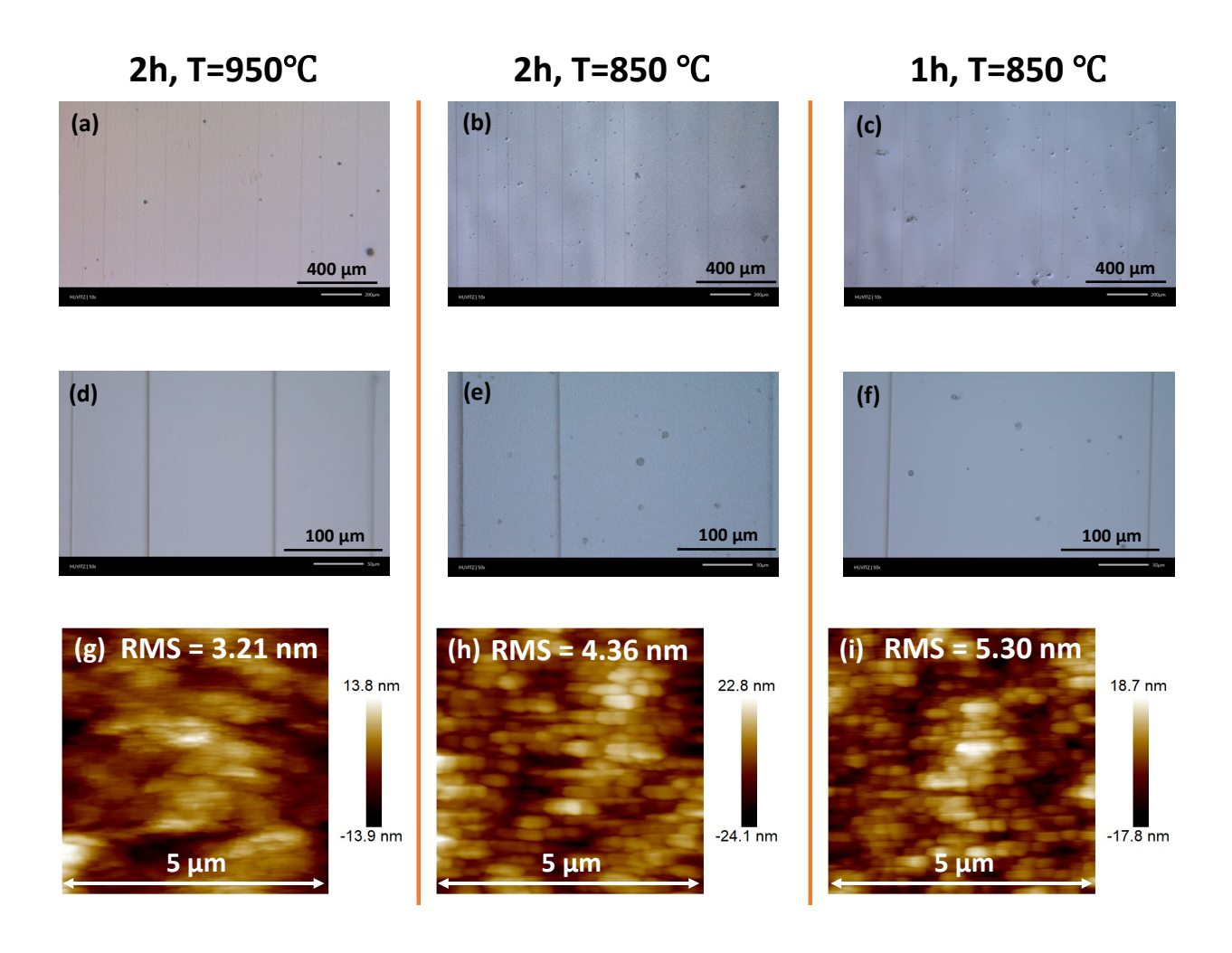


Fig 8. XRD ω -2θ patterns for β-Ga₂O₃ films grown with TMGa on (001) Sn-doped β-Ga₂O₃ substrates with different growth duration: (a) 0.5h (#10) and (b) 3h (#8).

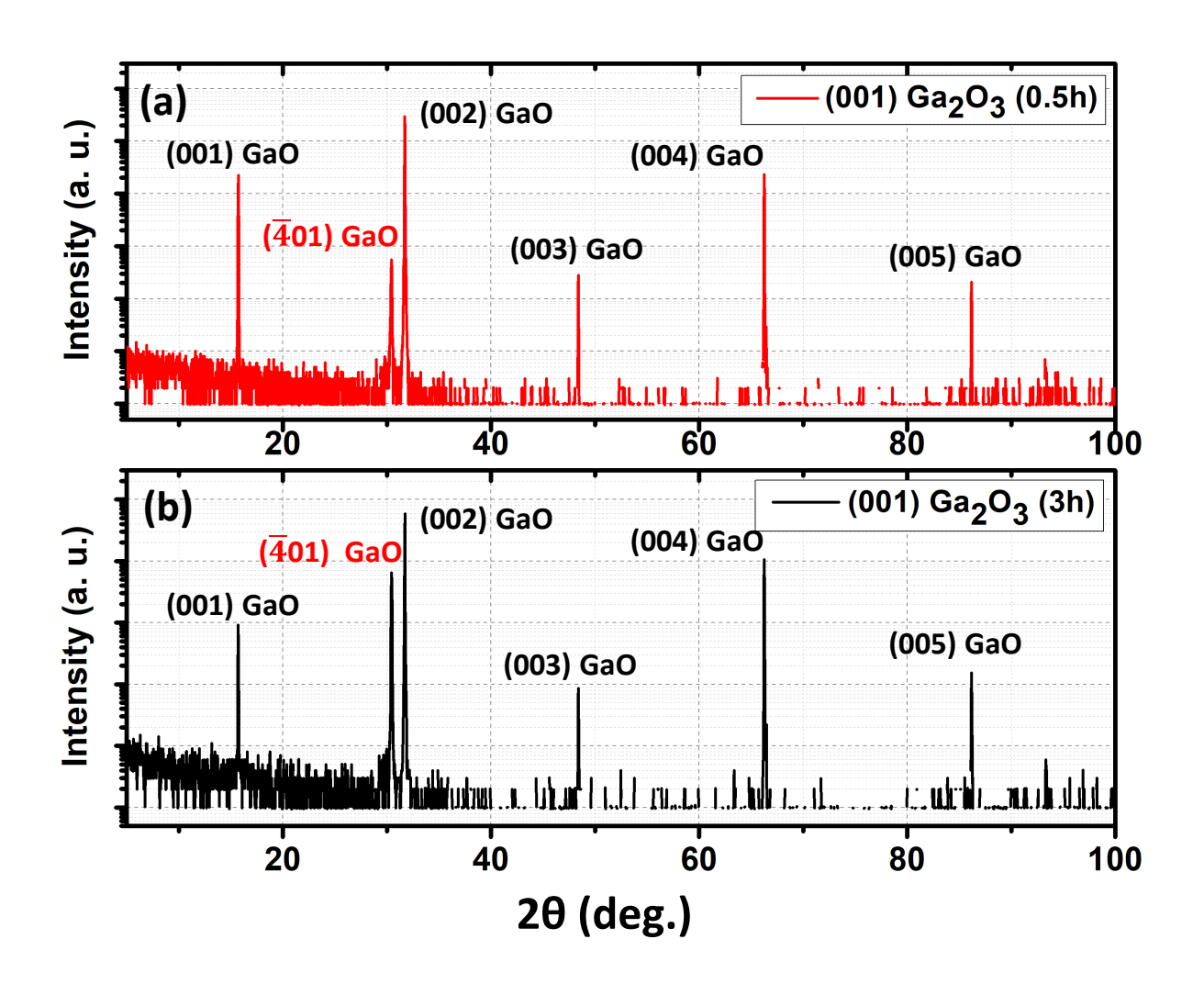


Fig 9. High resolution STEM images of β -Ga₂O₃ films grown with TMGa on (001) Sn-doped β -Ga₂O₃ substrate (#9) (a) The cracking in the film (b) zig zag at the interface and (c) high mag zig zag area and (d) rotation domains.

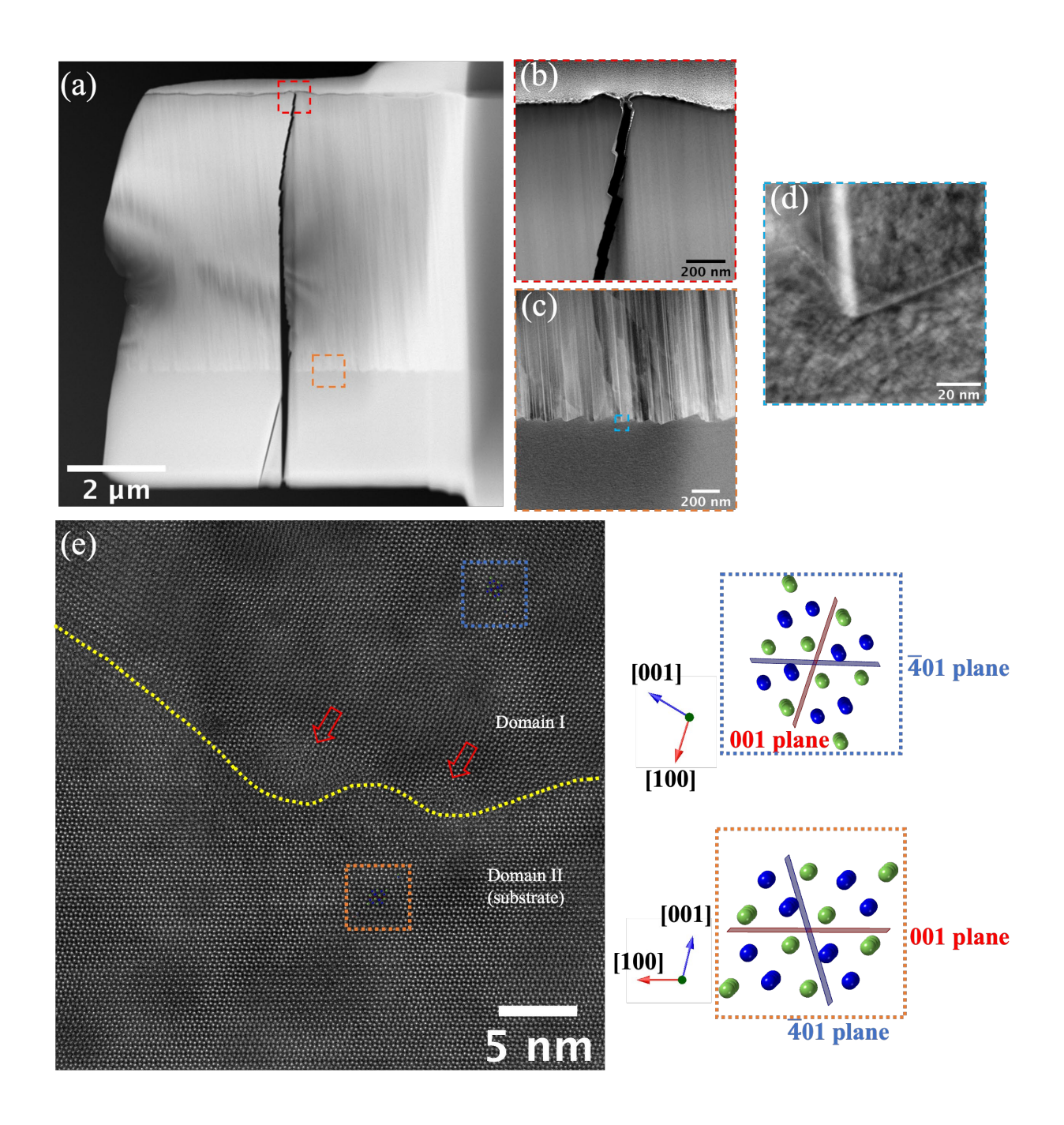
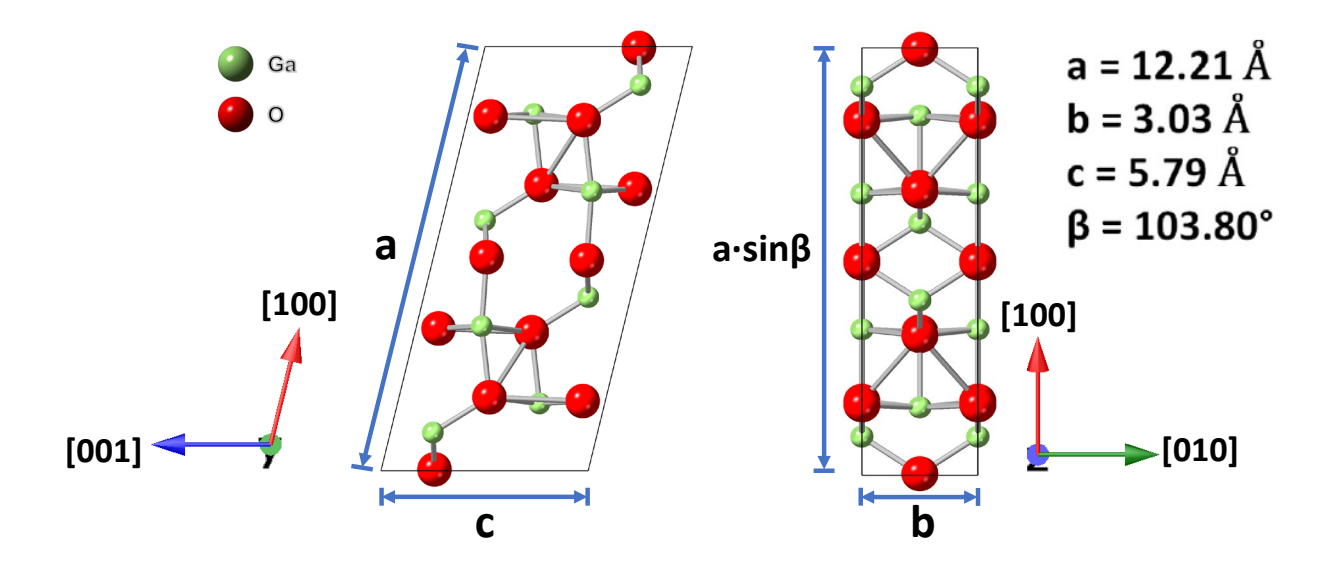


Fig 10. Crystal structure of β-Ga₂O₃ viewed in [010] (left) and [001] (right) directions.



For Table of Contents Use Only

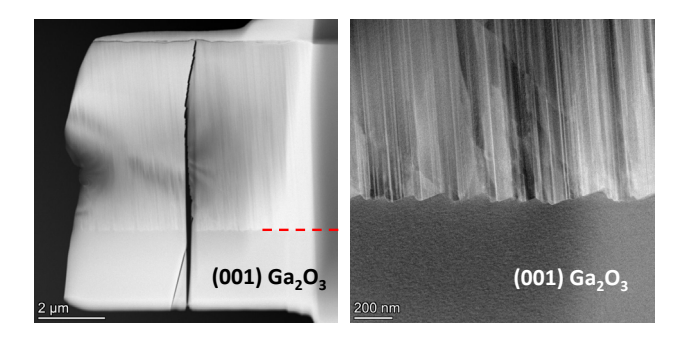
MOCVD growth of β-Ga₂O₃ on (001) Ga₂O₃ substrates

Lingyu Meng¹, Dongsu Yu¹, Hsien-Lien Huang², Chris Chae², Jinwoo Hwang², and Hongping Zhao^{1,2,‡}

¹Department of Electrical and Computer Engineering, The Ohio State University, Columbus, OH 43210, USA

²Department of Materials Science and Engineering, The Ohio State University, Columbus, OH 43210, USA

‡Corresponding Author Email: <u>zhao.2592@osu.edu</u>



MOCVD growth of β -Ga₂O₃ thin films on (001) on-axis Ga₂O₃ substrates revealed opportunity for thick film epitaxy using TMGa as the precursor. Smooth surface morphology is achievable but associated with cracks formation. Impurity carbon incorporation tends to be higher in films grown along (001) crystal orientation as compared to that in (010) β -Ga₂O₃ films.